Supplemental Material
Magnetic domain walls in strain-patterned ultrathin films

Aurore Finco, Marco Perini, André Kubetzka, Kirsten von Bergmann, and Roland Wiesendanger

Department of Physics, University of Hamburg, D-20355 Hamburg, Germany

Contrast mechanisms on domain walls with STM

Spin-polarized scanning tunneling microscopy allows to image magnetic structures exploiting the tunneling magnetoresistance (TMR) effect [1]: the tunnel current between a magnetic tip and a magnetic sample changes with the relative orientation of the directions of the magnetization at the apex of the tip and the local magnetization of the sample. In first approximation it is larger when these magnetizations are parallel than when they are anti-parallel. More generally, the tunnel current, and also the differential conductance ($\mathrm{d}I/\mathrm{d}U$), are proportional to the projection of the local sample magnetization onto the direction of the magnetization at the tip apex. Therefore, tips with an apex which is magnetized in the out-of-plane (in-plane) direction allow to observe the out-of-plane (in-plane) magnetization component of magnetic structures. Figures S1(b)-(d) show the contribution of the TMR to the $\mathrm{d}I/\mathrm{d}U$ in the case of two Néel walls with a unique rotational sense (Fig. S1(a)), for different tip sensitivities. When the tip is sensitive to the out-of-plane component of the magnetization, only the oppositely magnetized domains are visible (image (b)). When it is in-plane sensitive (here in the direction perpendicular to the wall), only the domain walls are visible and appear either bright or dark (image (c)). Figures 2(b) and 3(b) in the main text show $\mathrm{d}I/\mathrm{d}U$ measurements performed with either a fully in-plane sensitive magnetic tip or a tip with a canted

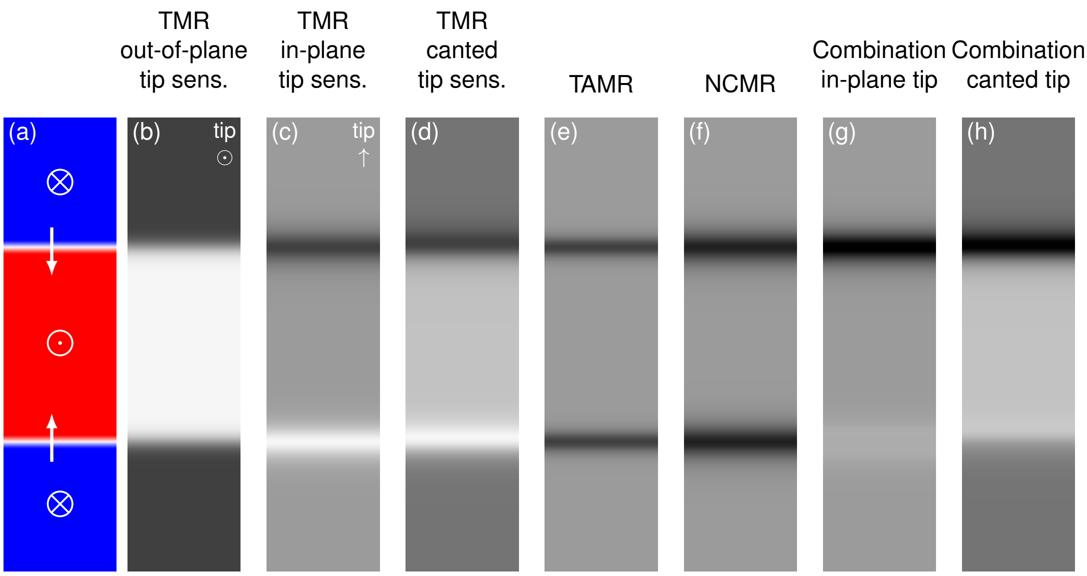

Figure S1: Sketch explaining the contrast observed in Figs. 2(b) and 3(b) in the case of two Néel walls with the same rotational sense (a). The images (b), (c) and (d) show the contrast induced by the tunneling magnetoresistance (TMR). In (b) the tip is sensitive to the out-of-plane component of the sample magnetization, while in (c) to the in-plane component, which is perpendicular to the wall. In image (d), the direction of the tip sensitivity is canted, in a position between the cases (b) and (c), showing both the out-of-plane and the in-plane components. Image (e) shows the contrast generated by the tunneling anisotropic magnetoresistance (TAMR) and image (f) the contribution of the non-collinear magnetoresistance (NCMR). Image (g) is a linear combination of the contributions (c), (e) and (f) reproducing the contrast in Fig. 2(b). Using the TMR contribution from image (d), a similar combination allows to reproduce the contrast from Fig. 3(b), as shown in image (h).

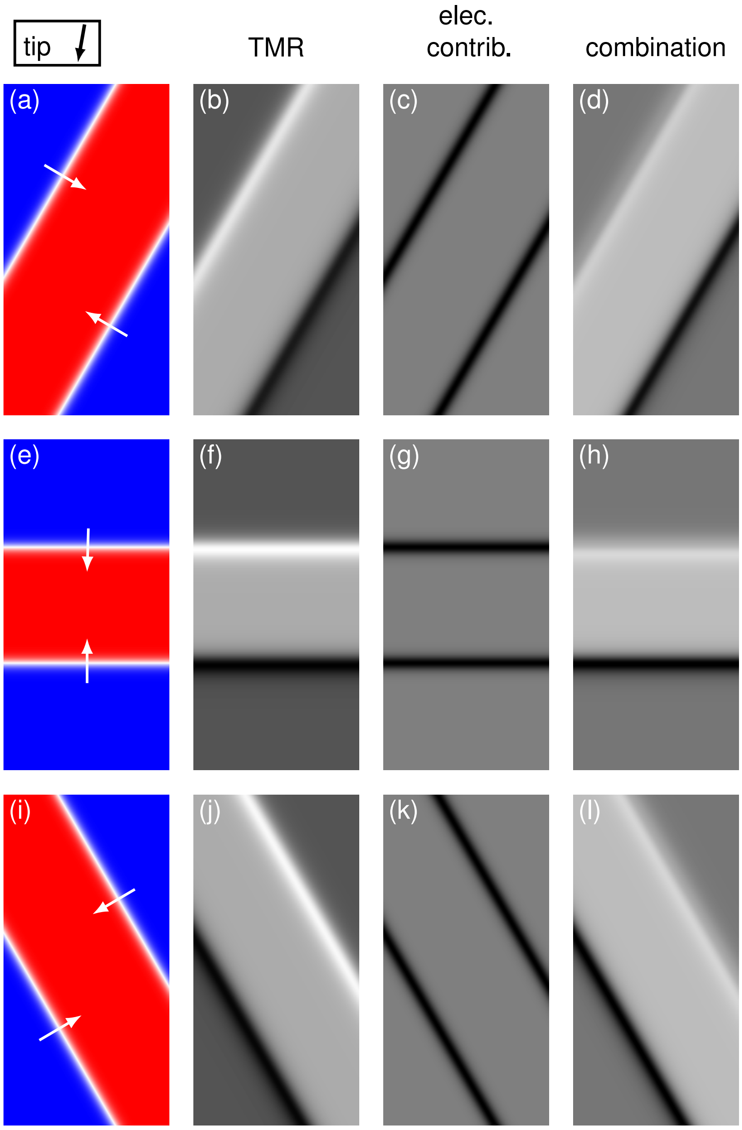

Figure S2: Sketch of the expected contrast for domain walls oriented along the three possible directions of the dislocation lines in Fig. 3(b) in the main text. The first column ((a), (e), (i)) shows the out-of-plane magnetization component for a pair of Néel walls with same rotational sense. The second column ((b), (f), (j)) displays the TMR contrast expected from these magnetic configurations for a tip with canted magnetic sensitivity, with in-plane direction indicated by the arrow on the top left corner. Panels (c), (g) and (k) show the contribution of the electronic effects to the measured signal, and the last column ((d), (h), (l)) represents the combination of TMR and electronic effects, corresponding to the signal measured in Fig. 3(b). The variation of contrast in the out-of-plane domains between the second and the last column is caused by changes in the color scale, which was adjusted separately for each column, to increase visibility of the walls' contrast.

sensitivity, the latter one showing both the out-of-plane and the in-plane component of the magnetic state (see Fig. S1(d)). However, the contrast observed in the experimental data does not look similar to what is shown in Figs. S1(b)-(d), indicating that the TMR is not the only source of contrast on the domain walls.
Non-collinear magnetic structures such as domain walls can also be imaged using non-magnetic tips, making use of electronic effects such as the tunneling anisotropic magnetoresistance (TAMR) [2] and the non-collinear magnetoresistance (NCMR) [3]. The TAMR produces a variation of the local density of states (LDOS) with the quantization axis of the sample magnetization, meaning that it is possible to distinguish out-of-plane and in-plane oriented sample areas. Also the NCMR produces a change in the LDOS, which is proportional to the degree of non-collinearity of the magnetic structure, i.e. the larger the angles between adjacent spins the larger the modification in the LDOS. In order to reproduce the contrast observed in Figs. 2(b) and 3(b), namely very dark walls alternating with hardly visible walls, we also need to model the contrast induced by the TAMR and the NCMR on domain walls, which of course can also have a con-

tribution in measurements with magnetic tips. We assume that the TAMR contribution to the $\mathrm{d}I/\mathrm{d}U$ scales with the uniaxial anisotropy energy density $K\cos^2(\varphi)$, where φ is the angle of the spins in the wall with respect to the magnetic easy axis. This is justified by the common origin of both the anisotropy and the change in LDOS due to the TAMR, which is the spin-orbit coupling [2]. The contrast induced by the NCMR at a specific atomic site i is assumed to be proportional to the mean nearest-neighbour angle, which is the average value of the magnetization angles between the site i and its six nearest neighbour sites [3]. Figures S1(e) and (f) show that the two walls of Fig. S1(a), when imaged via either the TAMR or the NCMR, present the same level of contrast, assumed negative in this example. Such contrast is thus independent of the wall's magnetization direction. From our experiments it is not possible to disentangle TAMR from NCMR. The contrast observed for the walls in Figs. 2(b) and 3(b) can be recovered by considering a combination of TMR, TAMR and NCMR. The TAMR and the NCMR reduce the $\mathrm{d}I/\mathrm{d}U$ signal at the position of the walls, which makes the dark walls appear darker and compensate the signal on the bright walls which become hardly visible, as illustrated in Fig. S1(g) and (h).

Figure S2 shows the expected signal for the domain walls in Fig. 3(b), which can be oriented along the three possible directions of the dislocation lines because of the strong pinning in Ni/Fe/Ir(111). The Figure displays the TMR contribution, the additional contrast induced by electronic effects, and their combination for three pairs of Néel domain walls, with same rotational sense, oriented in the three different directions. The TMR contribution is evaluated for a canted magnetic sensitivity of the tip, whose in-plane direction is indicated by the arrow. This direction is the same as in Fig. 3(b). Figures S2(d), (h) and (l), where TMR and electronic effects are combined, show that horizontal walls have a similar appearance to walls which are tilted by 60°. Additionally, walls which possess bright TMR contrast are now hardly distinguishable from the domains they separate. These results are in agreement with what has been observed for Fig. 3(b) in the main text.

Unique rotational sense of the domain walls in Co/Pt(111)

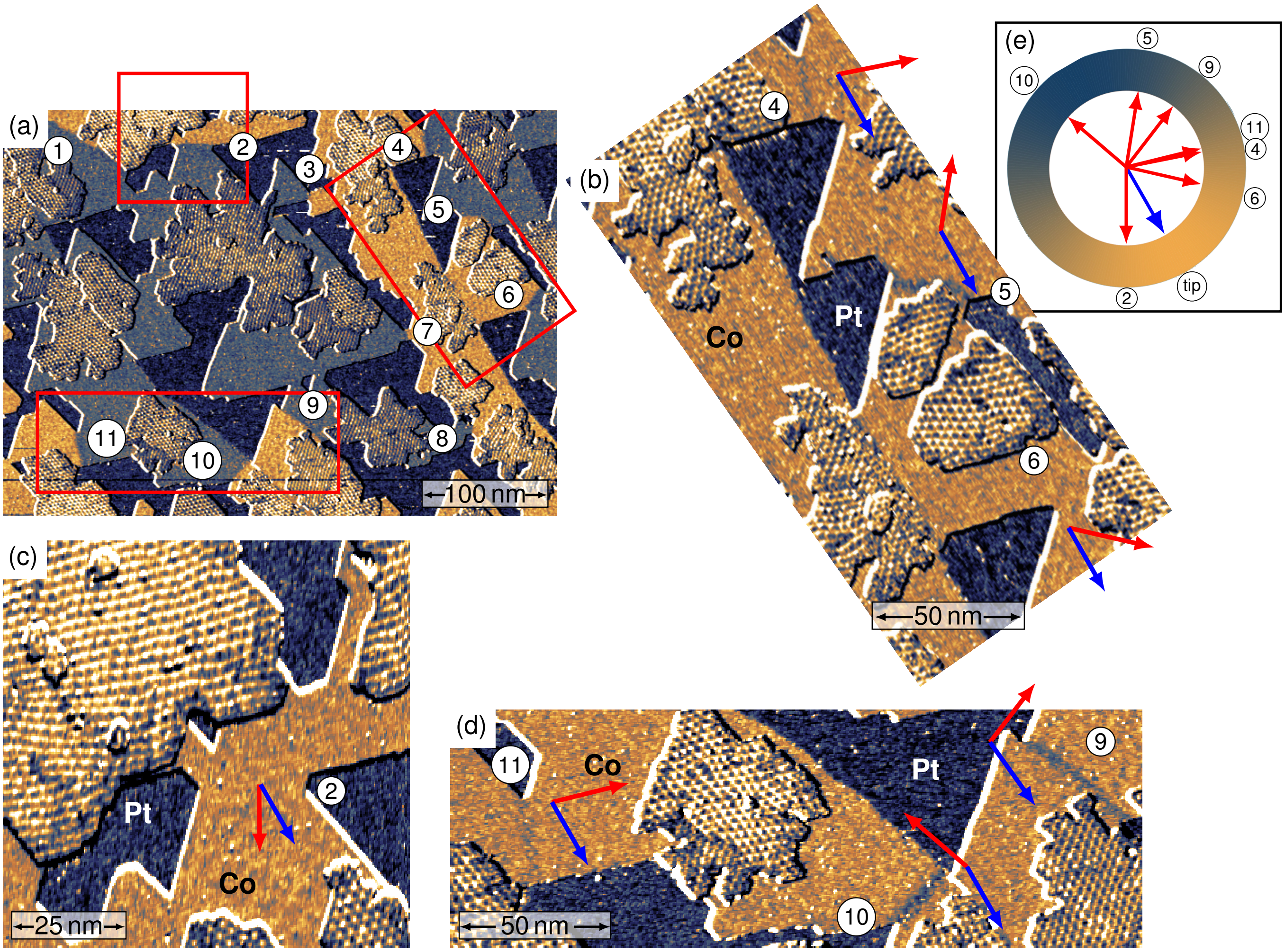

Figure S3: (a): Spin-resolved differential conductance map with out-of-plane sensitivity of a Co/Pt(111) sample, with several domain walls labelled by numbers. The red boxes indicate the areas shown in (b), (c) and (d). (b) to (d): Higher resolution images of domain walls in (a) using a tip sensitive to the in-plane magnetization component. The red arrows indicate the magnetic direction within the walls. The blue arrows indicate the tip magnetization direction. (e): Calculated TMR contrast as a function of the angle with respect to the tip magnetization direction (in blue). The directions of all the considered wall magnetizations are drawn in red and labelled by numbers. Measurement parameters: (a) to (d): 250 mV, 1 nA, 4 K, 0 T, Cr bulk tip.

Figure S3(a) shows several domain walls in Co/Pt(111), imaged with an out-of-plane sensitive magnetic tip and numbered from 1 to 11 (same data as Fig. 2(a) in the main text). To investigate whether all these walls have the same rotational sense, we have imaged some of them at higher resolution using an in-plane sensitive magnetic tip (Figs. S3(b) to (d)). Because we anticipate that the DMI at the Co/Pt interface might play a role for the magnetization within the walls, we assume that the walls are of Néel type and tentatively assign a unique rotational sense to them, which is selected arbitrarily to be a rotation from the bright to the dark magnetic domains. We then check if the magnetic contrast of the walls obtained with an in-plane tip is consistent with this hypothesis. For this analysis we have discarded wall number 1, since it moves between different positions while scanning across it, and walls number 3, 7 and 8 because they sit on constrictions whose size is comparable with the domain wall width, which can give rise to additional effects due to confinement [4] or edge effects [5].

No wall appears brighter than the adjacent domains, and therefore at the bias voltage we used we need to consider both TMR and electronic effects such as TAMR and NCMR as contrast mechanisms. We find that the additional electronic contribution reduces the $\mathrm{d}I/\mathrm{d}U$ signal at the walls' position, so that they appear similar to what is sketched in Fig. S1(g). The walls number 2 and 6 are hardly visible, i.e. in this case they are the walls with the highest $\mathrm{d}I/\mathrm{d}U$ signal. Walls number 4 and 11 have a slightly lower $\mathrm{d}I/\mathrm{d}U$ signal, followed by walls number 5 and 9, which are even darker. Wall number 10 has the lowest contrast level. We indicate the magnetization direction within the walls in Figs. S3(b) to (d) with red arrows. The tip magnetization direction is closest to the magnetization directions of the brightest walls, namely walls number 2 and 6. This means that the angle between tip and wall magnetization direction is the smallest for these two walls. Walls number 4 and 11 present a slightly lower $\mathrm{d}I/\mathrm{d}U$ contrast, and therefore we expect such angle to be larger than for walls 2 and 6. Similarly, the angle for walls number 5 and 9 will be even larger, given their darker $\mathrm{d}I/\mathrm{d}U$ contrast. Finally we expect the largest tip-wall angle, i.e. the closest to 180°, for wall number 10. The tip magnetization direction derived in this way is sketched by the blue arrow. All the observed $\mathrm{d}I/\mathrm{d}U$ contrast levels of the walls are in accordance with the proposed magnetization direction within the walls, as sketched in Fig. S3(e), demonstrating that our assumption of fixed sense of magnetization rotation is correct. Note that this conclusion also holds if we assume the opposite wall rotational sense, namely from dark to bright magnetic domains, by simply considering a tip direction rotated by 180° in the sample plane.

References

[1] R. Wiesendanger. Spin mapping at the nanoscale and atomic scale. *Rev. Mod. Phys.* 81 (2009), 1495–1550.

[2] M. Bode, S. Heinze, A. Kubetzka, O. Pietzsch, X. Nie, G. Bihlmayer, S. Blügel, and R. Wiesendanger. Magnetization-Direction-Dependent Local Electronic Structure Probed by Scanning Tunneling Spectroscopy. *Phys. Rev. Lett.* 89 (2002), 237205.

[3] C. Hanneken, F. Otte, A. Kubetzka, B. Dupé, N. Romming, K. von Bergmann, R. Wiesendanger, and S. Heinze. Electrical detection of magnetic skyrmions by tunnelling non-collinear magnetoresistance. *Nat. Nanotech.* 10 (2015), 1039–1042.

[4] P. Bruno. Geometrically Constrained Magnetic Wall. *Phys. Rev. Lett.* 83 (1999), 2425–2428.

[5] S. Rusponi, T. Cren, N. Weiss, M. Epple, P. Buluschek, L. Claude, and H. Brune. The remarkable difference between surface and step atoms in the magnetic anisotropy of two-dimensional nanostructures. *Nat. Mater.* 2 (2003), 546–551.